795

VOLUME 81 PAPER No. 795

PROCEEDINGS

AMERICAN SOCIETY
OF
CIVIL ENGINEERS

SEPTEMBER, 1955

ELASTIC INSTABILITY OF FLAT PLATES SUBJECTED TO PARTIAL EDGE LOADS

by Lev Zetlin, A.M. ASCE

ENGINEERING MECHANICS
DIVISION

{Discussion open until January 1, 1956}

Copyright 1955 by the AMERICAN SOCIETY OF CIVIL ENGINEERS
Printed in the United States of America

Headquarters of the Society
33 W. 39th St.
New York 18, N. Y.

PRICE $0.50 PER COPY

THIS PAPER

--represents an effort by the Society to deliver technical data direct from the author to the reader with the greatest possible speed. To this end, it has had none of the usual editing required in more formal publication procedures.

Readers are invited to submit discussion applying to current papers. For this paper the final date on which a discussion should reach the Manager of Technical Publications appears on the front cover.

Those who are planning papers or discussions for "Proceedings" will expedite Division and Committee action measurably by first studying "Publication Procedure for Technical Papers" (Proceedings Paper No. 290). For free copies of this Paper—describing style, content, and format—address the Manager, Technical Publications, ASCE.

Reprints from this publication may be made on condition that the full title of paper, name of author, page reference, and date of publication by the Society are given.

The Society is not responsible for any statement made or opinion expressed in its publications.

This paper was published at 1745 S. State Street, Ann Arbor, Mich., by the American Society of Civil Engineers. Editorial and General Offices are at 33 West Thirty-ninth Street, New York 18, N. Y.

ELASTIC INSTABILITY OF FLAT PLATES SUBJECTED TO PARTIAL EDGE LOADS[1]

Lev Zetlin,[2] A.M. ASCE

SYNOPSIS

Buckling loads are determined of flat rectangular plates subject to loads distributed over short portions of the edges. The equations governing the buckling loads, which are partial differential equations with variable coefficients, are discussed and an approach to the solution is made by means of the Energy Method. Results of calculations have been reduced to curves suitable for design purposes. These curves are given for a wide range of plate dimensions and loading widths. The theoretical results are compared with a number of tests.

Notation

- L - the horizontal length (span) of plate.
- h - the vertical height (depth) of plate.
- β - h/L; non-dimensional ratio.
- t - thickness of plate.
- $2B$ - width through which the external load is applied to the top edge of plate.
- σ_x - stress in the x-direction.
- σ_y - stress in the y-direction.
- τ_{xy} - shearing stress
- σ_Y - yield stress in the steel of the test specimen.
- A_n, B_n, C_n, and D_n - coefficients in the stress function.
- A_{mk} or A_{pr} - (or A with any numerical subscript), amplitudes of the double Fourier series in the eigenfunction.
- D - flexural rigidity.
- $w(x,y)$ - displacement of a point anywhere on the neutral plane of the plate in the direction perpendicular to the plane of the plate.

---

1. Based on a thesis by L. Zetlin submitted to Cornell University in June 1953 in partial fulfillment of the requirements for the degree of Doctor of Philosophy.
2. Asst. Prof., Structural Engineering, Cornell University, Ithaca, N. Y.

INTRODUCTION

This paper presents an analysis of the elastic stability of a plate supported at both ends and loaded over a portion of one of the edges. The plate is shown in Fig. 1. Its edges are simply supported. The total edge load, P, is applied along the top edge and is uniformly distributed over a width 2B with intensity p = P/2B. The reactions are supplied by shear stresses with parabolic distribution along the two vertical edges. Both the reactions and the external load P are symmetrical about the center line of the plate. The solution is for the critical value of p at which the plate buckles and is in terms of the three parameters, β = h/L, 2B and D. Thus, the solution applies to a wide range of variations in the dimensions of the plate and width of the strip loading. This small deflection analysis is based on the usual assumptions of elasticity, homogeneity and isotropy.

Since the mathematical form of the solution is too complex for direct use by a designer, a number of graphs have been drawn from which the buckling loads can be easily read.

To the author's best knowledge, the only investigation of a somewhat similar problem is that by K. Girkmann.[2,3,4] His results however, apply only to plates with $h/L \geq 0.9$, because of certain mathematical limitations in his initial assumptions. This will be pointed out more explicitly later in connection with the mathematical development of the problem. Moreover, Professor Girkmann's papers give the solution only in the form of a determinant, which has to be evaluated for any particular case.

Only the most essential mathematical steps and results, which are necessary for the understanding of the theoretical procedure in the solution of the problem, are given in this paper. For the complete mathematical development of the solution the reader is referred to footnote 1.

I. Theoretical Solution

The elastic instability of any flat plate is governed by the eigenvalues of the following differential equation (see for instance Ref. 1, page 324):

$$\frac{\partial^4 w}{\partial x^4} + 2\frac{\partial^4 w}{\partial x^2 \partial y^2} + \frac{\partial^4 w}{\partial y^4} = \frac{1}{D}\left\{\sigma_x t \frac{\partial^2 w}{\partial x^2} + \sigma_y t \frac{\partial^2 w}{\partial y^2} + 2\tau_{xy} t \frac{\partial^2 w}{\partial x \partial y}\right\}$$

Eqn. (1)

The coefficients of the derivatives on the right-hand side of Eqn. (1) are stresses throughout the plate due to the external loads; these stresses are in the plane of the plate and are assumed to be constant through the thickness of the plate. Obviously, for the case shown in Fig. 1 the stresses vary from

point to point in the plane of the plate and the differential equation (1) is one with variable coefficients.

In order to be able to cope with Eqn. (1), the stress distribution throughout the plate has to be determined first. Since a solution in terms of plate dimensions and width of the strip loading as parameters is desired, the stresses have to be given as functions of the coordinates (xy).

a) Stress Distribution in the Plate.

The stress distribution in the plate of Fig. 1 due to the external loads as shown, can be determined by the following stress function taken from Ref. (2) and (5):

$$\Phi = \sum_{n=1,3,5\ldots}^{\infty} \frac{L^2}{n\pi^2} \left\{ A_n e^{n\pi\tilde{y}/L} + B_n e^{-n\pi\tilde{y}/L} + C_n \frac{n\pi\tilde{y}}{L} e^{n\pi\tilde{y}/L} + D_n \frac{n\pi\tilde{y}}{L} e^{-n\pi\tilde{y}/L} \right\} \cos \frac{n\pi\tilde{x}}{L}$$

Eqn. (2)

where A_n, B_n, C_n and D_n are constants which depend on the boundary forces along the horizontal edges of the plate. The shear stress distribution along the vertical edges resulting from this stress function is close to parabolic.

Along the top edge, the external load p = P/2B is expanded in a Fourier series.

$$p(x) = \frac{4p}{\pi} \sum_{n=1,3,5\ldots}^{\infty} \frac{1}{n} \sin \frac{n\pi B}{L} \cos \frac{n\pi\tilde{x}}{L} = \sum_{n=1,3,5\ldots}^{\infty} p_n \cos \frac{n\pi\tilde{x}}{L}$$

Eqn. (3)

The boundary conditions on the stresses are:

at y = 0; $\tau_{xy} = 0$ . . . . . Eqn. (4a) and $\sigma_y = -\frac{p(x)}{t}$ . . . . . Eqn. (4b)

at y = h; $\tau_{xy} = 0$ . . . . . Eqn. (4c) and $\sigma_y = 0$ . . . . . Eqn. (4d)

Differentiation of Eqn. (2) as is indicated below, together with the proper substitution of the boundary stresses of Eqns (4), yield the following expressions for the stresses in the plate.

$$\sigma_x = \frac{\partial^2 \Phi}{\partial y^2} = \sum_{n=1,3,5\ldots}^{\infty} \left\{ (A_n + 2C_n) e^{n\pi\tilde{y}/L} + (B_n - 2D_n) e^{-n\pi\tilde{y}/L} + C_n \frac{n\pi\tilde{y}}{L} e^{n\pi\tilde{y}/L} + D_n \frac{n\pi\tilde{y}}{L} e^{-n\pi\tilde{y}/L} \right\} \cos \frac{n\pi\tilde{x}}{L}$$

Eqn. (5a)

$$\sigma_y = \frac{\partial^2 \Phi}{\partial x^2} = -\sum_{n=1,3,5\ldots}^{\infty} \left\{ A_n e^{n\pi\tilde{y}/L} + B_n e^{-n\pi\tilde{y}/L} + C_n \frac{n\pi\tilde{y}}{L} e^{n\pi\tilde{y}/L} + D_n \frac{n\pi\tilde{y}}{L} e^{-n\pi\tilde{y}/L} \right\} \cos \frac{n\pi\tilde{x}}{L}$$

Eqn. (5b)

$$\tau_{xy} = -\frac{\partial}{\partial x}\left(\frac{\partial \Phi}{\partial y}\right) = \sum_{n=1,3,5\ldots}^{\infty} \left\{ (A_n + C_n) e^{n\pi\tilde{y}/L} - (B_n - D_n) e^{-n\pi\tilde{y}/L} + C_n \frac{n\pi\tilde{y}}{L} e^{n\pi\tilde{y}/L} - D_n \frac{n\pi\tilde{y}}{L} e^{-n\pi\tilde{y}/L} \right\} \sin \frac{n\pi\tilde{x}}{L}$$

Eqn. (5c)

The constants A_n, B_n, C_n and D_n in Eqn. (5) (which are the same constants as in Eqn. (2)) are given by Eqn. (6) below:

$$A_n = -\rho_n K_n \left[\left(1 + 2n\tilde{\pi}\beta + 2n^2\tilde{\pi}^2\beta^2\right) e^{-2n\tilde{\pi}\beta} - e^{-4n\tilde{\pi}\beta} \right]$$

$$B_n = \rho_n K_n \left[1 - \left(1 - 2n\tilde{\pi}\beta + 2n^2\tilde{\pi}^2\beta^2\right) e^{-2n\tilde{\pi}\beta} \right]$$

$$C_n = \rho_n K_n \left[\left(1 + 2n\tilde{\pi}\beta\right) e^{-2n\tilde{\pi}\beta} - e^{-4n\tilde{\pi}\beta} \right]$$

$$D_n = \rho_n K_n \left[1 - \left(1 - 2n\tilde{\pi}\beta\right) e^{-2n\tilde{\pi}\beta} \right]$$

Eqn. (6)

where

$$K_n = \frac{1}{t} \cdot \frac{1}{1 - 2\left(1 + 2n^2\tilde{\pi}^2\beta^2\right) e^{-2n\pi\beta} + e^{-4n\tilde{\pi}\beta}}$$

Eqn. (7)

b) Determination of the Buckling Load.

Having expressions for the stresses in Eqns. (5), one way to determine the critical load p is to substitute Eqns. (5) into Eqn. (1); then, one of the eigenvalues of Eqn. (1) would yield the critical load, probably in the form of an infinite series. The mathematical background on which such a procedure should be based, as well as a discussion of a mathematical proof that a solution to Eqn. (1) exists, is treated at some length in footnote 1. Such a procedure, however, if at all practically possible, would be an ambitious undertaking.

Another, more practical way, to determine the critical load p, is the use of energy relationships of the plate at buckling, and subsequent application of the Rayleigh-Ritz method. This procedure, too, is discussed extensively in footnote 1, and its explanation is beyond the scope of this paper. Only the essential steps and equations of this procedure will be pointed out below.

If at the instant that the plate passes from stable to unstable equilibrium, ΔU denotes the increment of the total potential energy of the plate and the external loads, ΔV denotes the increment of the strain energy of the plate,

and ΔT denotes the increment of the potential energy of the external loads, then:

$$\Delta U = \Delta V + \Delta T \qquad \ldots\ldots \text{Eqn.(8)}$$

Expressing ΔV and ΔT in terms of plate dimensions, its material properties, and the stresses in the plate, the following relationship results:

$$\Delta U = \frac{D}{2}\int_0^h \int_{-L/2}^{L/2} \left\{ \left(\frac{\partial^2 w}{\partial x^2} + \frac{\partial^2 w}{\partial y^2}\right)^2 - 2(1-\nu)\left[\frac{\partial^2 w}{\partial x^2}\frac{\partial^2 w}{\partial y^2} - \left(\frac{\partial^2 w}{\partial x \partial y}\right)^2\right]\right\} dx\,dy$$

$$+ \frac{t}{2}\int_0^h \int_{-L/2}^{L/2} \left\{ \sigma_x \left(\frac{\partial w}{\partial x}\right)^2 + \sigma_y \left(\frac{\partial w}{\partial y}\right)^2 + 2\tilde{\tau}_{xy}\frac{\partial w}{\partial x}\frac{\partial w}{\partial y}\right\} dx\,dy$$

Eqn. (9)

An expression similar to Eqn. (9) can be found on page 325 of Ref. (1) and its derivation on pages 311-314 of the same reference.

Stresses σ_x, σ_y and $\tilde{\tau}_{xy}$ in Eqn. (9) are, of course, given by Eqns. (5). In order to be able to proceed with the solution of the problem, an expression for w as a function of x and y, i.e. the deflected shape of the plate at buckling, should be known or properly assumed. The closer the assumption is to the actual buckled shape of the plate, the closer will be the computed critical load p to the actual buckling load.

In this respect, the author had the advantage of tests on a related problem before the theoretical solution was attempted. From these tests, observations of the shape of the plate at failure had been made. The tests will be discussed in more detail later in the paper.

The available test observations indicated qualitatively that the shape of such plates at failure, for a large range of variations in the parameters 2B, and h/L, could be represented with good accuracy by the following trigonometric series:

$$w(x,y) = \sum_{m=1,2} \sum_{\kappa=1,3,5} A_{m\kappa} \sin\frac{m\pi y}{h} \cos\frac{\kappa\pi x}{L}$$

Eqn. (10) *

where A_{mk} are constants to be determined by the Rayleigh-Ritz method.

That the assumption in Eqn. (10) is satisfactory, will be demonstrated

* It will be noticed that Eqn. (10) satisfies the boundary conditions of the plate in Fig. 1.

later in comparing computed critical loads with the failure loads observed in the tests.

At this stage the reader will be referred to the statement made in the Introduction in connection with the limitation of Professor Girkmann's work. Professor Girkmann[2] assumed the following expression for w:

$$w(x,y)=\left[A\sin\frac{\tilde{\pi}y}{h}+B\sin\frac{2\tilde{\pi}y}{h}+C\sin\frac{3\tilde{\pi}y}{h}\right]\cos\left(\frac{\tilde{\pi}x}{L}\right)$$

Eqn. (11)

Eqn. (11) has more limited possibilities to represent the shape of a buckled plate than Eqn. (10). Hence, the critical loads yielded by Eqn. (11) are likely to be less accurate than those yielded by Eqn. (10). This will be particularly so with smaller values of h/L (i.e. longer plates) and smaller values of 2B (width of the strip loading).

The next step is to evaluate the increment of the total potential energy ΔU in Eqn. (9). For this purpose, Eqn. (10) is differentiated as indicated by Eqn. (9); the differentiated expressions and the expressions for the stresses as given by Eqns. (5) are substituted into Eqn. (9), and, finally, integration of Eqn. (9) is performed. The process is quite lengthy and its details will not be given here. It will be found in footnote 1. The described operation gives an expression for ΔU in terms of the parameters 2B, h/L and D, and the six unknown constants A_{mk}.

Since the total potential energy at elastic instability has a stationary value, $\partial(\Delta U)/\partial A_{mk} = 0$. Hence, in the final step of the solution, ΔU is differentiated with respect to each of the six constants A_{mk} and each derivative is equated to zero. Thus, six homogeneous algebraic equations in the six unknowns A_{mk} (i.e. A_{11}, A_{13}, A_{15}, A_{21}, A_{23}, A_{25}) are obtained. These equations have the following form:

$$\frac{\partial(\Delta U)}{\partial A_{11}}=\left[\Gamma_1+\frac{\lambda}{P}\overline{\Pi}_1\right]A_{11}+\frac{\Gamma_7}{2}A_{13}+\frac{\Gamma_8}{2}A_{15}+\frac{\Gamma_9}{2}A_{21}+\frac{\Gamma_{10}}{2}A_{23}+\frac{\Gamma_{11}}{2}A_{25}=0$$

$$\frac{\partial(\Delta U)}{\partial A_{13}}=\frac{\Gamma_7}{2}A_{11}+\left[\Gamma_2+\frac{\lambda}{P}\overline{\Pi}_2\right]A_{13}+\frac{\Gamma_{12}}{2}A_{15}+\frac{\Gamma_{13}}{2}A_{21}+\frac{\Gamma_{14}}{2}A_{23}+\frac{\Gamma_{15}}{2}A_{25}=0$$

$$\frac{\partial(\Delta U)}{\partial A_{15}}=\frac{\Gamma_8}{2}A_{11}+\frac{\Gamma_{12}}{2}A_{13}+\left[\Gamma_3+\frac{\lambda}{P}\overline{\Pi}_3\right]A_{15}+\frac{\Gamma_{16}}{2}A_{21}+\frac{\Gamma_{17}}{2}A_{23}+\frac{\Gamma_{18}}{2}A_{25}=0$$

$$\frac{\partial(\Delta U)}{\partial A_{21}}=\frac{\Gamma_9}{2}A_{11}+\frac{\Gamma_{13}}{2}A_{13}+\frac{\Gamma_{16}}{2}A_{15}+\left[\Gamma_4+\frac{\lambda}{P}\overline{\Pi}_4\right]A_{21}+\frac{\Gamma_{19}}{2}A_{23}+\frac{\Gamma_{20}}{2}A_{25}=0$$

$$\frac{\partial(\Delta W)}{\partial A_{23}} = \frac{\Gamma_{10}}{2}A_{11} + \frac{\Gamma_{14}}{2}A_{13} + \frac{\Gamma_{17}}{2}A_{15} + \frac{\Gamma_{19}}{2}A_{21} + \left[\Gamma_5 + \frac{\lambda}{p}\Pi_5\right]A_{23} + \frac{\Gamma_{21}}{2}A_{25} = 0$$

$$\frac{\partial(\Delta W)}{\partial A_{25}} = \frac{\Gamma_{11}}{2}A_{11} + \frac{\Gamma_{15}}{2}A_{13} + \frac{\Gamma_{18}}{2}A_{15} + \frac{\Gamma_{20}}{2}A_{21} + \frac{\Gamma_{21}}{2}A_{23} + \left[\Gamma_6 + \frac{\lambda}{p}\Pi_6\right]A_{25} = 0$$

Eqn. (12a)

In Eqn. (12a),

p is the external load, ...(12b)

$\lambda = \pi^4 \, D/L^2$ .....(12c)

$\pi_1, \pi_2, \ldots \pi_6$ are expressions which depend on β only. π_1, for example, is as follows:

$$\Pi_1 = \left[\frac{1}{8\beta^3}(\beta^2+1)^2\right]$$

Eqn. (12d)

$\Gamma_1, \Gamma_2, \ldots \Gamma_{21}$, are expressions in the form of infinite series which depend both on β and 2B. The expressions for Γ are quite lengthy; to give an idea of their form, Γ_1 is reproduced below:

$$\Gamma_1 = \frac{t}{p}\left\{\left[\sum_{n=1,3,5\ldots}^{\infty} 4(A_n+2C_n)\sin\frac{n\tilde{\imath}\imath}{2}\cdot\frac{(n^2-2)}{n^2(n^2-4)}\cdot\frac{1}{(n^2\beta^2+4)}\left(e^{n\tilde{\imath}\imath\beta}-1\right)\right]\right.$$

$$-\left[\sum_{n=1,3,5\ldots}^{\infty} 4(B_n-2D_n)\sin\frac{n\tilde{\imath}\imath}{2}\cdot\frac{(n^2-2)}{n^2(n^2-4)}\cdot\frac{1}{(n^2\beta^2+4)}\left(e^{-n\tilde{\imath}\imath\beta}-1\right)\right]$$

$$+\left[\sum_{n=1,3,5\ldots}^{\infty} 4C_n\sin\frac{n\tilde{\imath}\imath}{2}\cdot\frac{(n^2-2)}{n^2(n^2-4)}\cdot\frac{1}{(n^2\beta^2+4)}\left(n\tilde{\imath}\imath\beta e^{-n\tilde{\imath}\imath\beta}-\frac{(3n^2\beta^2+4)}{(n^2\beta^2+4)}\left(e^{n\tilde{\imath}\imath\beta}-1\right)\right)\right]$$

$$\left.+\left[\sum_{n=1,3,5\ldots}^{\infty} 4D_n\sin\frac{n\tilde{\imath}\imath}{2}\cdot\frac{(n^2-2)}{n^2(n^2-4)}\cdot\frac{1}{(n^2\beta^2+4)}\left(-n\tilde{\imath}\imath\beta e^{-n\tilde{\imath}\imath\beta}+\frac{(3n^2\beta^2+4)}{(n^2\beta^2+4)}\left(1-e^{-n\tilde{\imath}\imath\beta}\right)\right)\right]\right.$$

$$+\left[\sum_{n=1,3,5\ldots}^{\infty} 4A_n \sin\frac{n\tilde{\pi}}{2}\,\frac{1}{n^2(n^2-4)}\,\frac{(n^2\beta^2+2)}{\beta^2(n^2\beta^2+4)}\left(e^{n\tilde{\pi}\beta}-1\right)\right]$$

$$-\left[\sum_{n=1,3,5\ldots}^{\infty} 4B_n \sin\frac{n\tilde{\pi}}{2}\,\frac{1}{n^2(n^2-4)}\,\frac{(n^2\beta^2+2)}{\beta^2(n^2\beta^2+4)}\left(e^{-n\tilde{\pi}\beta}-1\right)\right]$$

$$+\left[\sum_{n=1,3,5\ldots}^{\infty} 4C_n \sin\frac{n\tilde{\pi}}{2}\,\frac{1}{n^2(n^2-4)}\,\frac{(n^2\beta^2+2)}{\beta^2(n^2\beta^2+4)}\left(n\tilde{\pi}\beta e^{n\tilde{\pi}\beta}-\frac{(n^4\beta^4+2n^2\beta^2+8)(e^{n\tilde{\pi}\beta}-1)}{(n^2\beta^2+2)(n^2\beta^2+4)}\right)\right]$$

$$+\left[\sum_{n=1,3,5\ldots}^{\infty} 4D_n \sin\frac{n\tilde{\pi}}{2}\,\frac{1}{n^2(n^2-4)}\,\frac{(n^2\beta^2+2)}{\beta^2(n^2\beta^2+4)}\left(-n\tilde{\pi}\beta e^{-n\tilde{\pi}\beta}+\frac{(n^4\beta^4+2n^2\beta^2+8)(1-e^{-n\tilde{\pi}\beta})}{(n^2\beta^2+2)(n^2\beta^2+4)}\right)\right]$$

$$+\left[\sum_{n}^{\infty} 4(A_n+C_n)\sin\frac{n\tilde{\pi}}{2}\,\frac{1}{(n^2-4)}\,\frac{1}{(n^2\beta^2+4)}\left(e^{n\tilde{\pi}\beta}-1\right)\right]$$

$$-\left[\sum_{n=1,3,5\ldots}^{\infty} 4(B_n-D_n)\sin\frac{n\tilde{\pi}}{2}\,\frac{1}{(n^2-4)}\,\frac{1}{(n^2\beta^2+4)}\left(e^{-n\tilde{\pi}\beta}-1\right)\right]$$

$$+\left[\sum_{n=1,3,5\ldots}^{\infty} 4C_n \sin\frac{n\tilde{\pi}}{2}\,\frac{1}{(n^2-4)}\,\frac{1}{(n^2\beta^2+4)}\left(n\tilde{\pi}\beta e^{n\tilde{\pi}\beta}-\frac{(e^{n\tilde{\pi}\beta}-1)2n^2\beta^2}{(n^2\beta^2+4)}\right)\right]$$

$$-\left[\sum_{n=1,3,5\ldots}^{\infty} 4D_n \sin\frac{n\tilde{\pi}}{2}\,\frac{1}{(n^2-4)}\,\frac{1}{(n^2\beta^2+4)}\left(n\tilde{\pi}\beta e^{-n\tilde{\pi}\beta}-\frac{(1-e^{-n\tilde{\pi}\beta})2n^2\beta^2}{(n^2\beta^2+4)}\right)\right]$$

Eqn. (12e)

It will be noted that the unknowns in Eqn. (12a) are the constants A_{mk} and the external load p.

The information that equations (12a) can supply is:

1) Values of p for which the set of the six equations in (12a) has non zero solutions for the A's. There will be, in general, six such distinct values of p, the smallest of which is the first buckling load.
2) Ratio between the six constants A_{mk}. If this ratio is known for any particular plate (i.e. certain values of 2B, h/L and D), the shape of the buckled plate can be represented by substituting the ratios of A_{mk} into Eqn. (10). Of course, as is the case in all instability problems, the actual deflections w will remain indeterminate as to magnitude.

Of the above two items, the first one is of practical interest. The second item may be of interest in research work as a check on the initial assumption of the buckled surface (Eqn. (10)).

In solving equations (12a), the smallest value of p has to be determined first; the corresponding ratios between A_{mk} can then be determined. For the set of the six equations (12a) to have solutions, the determinant of these equations has to be equal to zero, or:

$$\begin{vmatrix}
\left[\Gamma_1+\frac{\lambda}{p}\overline{\Pi}_1\right] & \frac{\Gamma_7}{2} & \frac{\Gamma_8}{2} & \frac{\Gamma_9}{2} & \frac{\Gamma_{10}}{2} & \frac{\Gamma_{11}}{2} \\
\frac{\Gamma_7}{2} & \left[\Gamma_2+\frac{\lambda}{p}\overline{\Pi}_2\right] & \frac{\Gamma_{12}}{2} & \frac{\Gamma_{13}}{2} & \frac{\Gamma_{14}}{2} & \frac{\Gamma_{15}}{2} \\
\frac{\Gamma_8}{2} & \frac{\Gamma_{12}}{2} & \left[\Gamma_3+\frac{\lambda}{p}\overline{\Pi}_3\right] & \frac{\Gamma_{16}}{2} & \frac{\Gamma_{17}}{2} & \frac{\Gamma_{18}}{2} \\
\frac{\Gamma_9}{2} & \frac{\Gamma_{13}}{2} & \frac{\Gamma_{16}}{2} & \left[\Gamma_4+\frac{\lambda}{p}\overline{\Pi}_4\right] & \frac{\Gamma_{19}}{2} & \frac{\Gamma_{20}}{2} \\
\frac{\Gamma_{10}}{2} & \frac{\Gamma_{14}}{2} & \frac{\Gamma_{17}}{2} & \frac{\Gamma_{19}}{2} & \left[\Gamma_5+\frac{\lambda}{p}\overline{\Pi}_5\right] & \frac{\Gamma_{21}}{2} \\
\frac{\Gamma_{11}}{2} & \frac{\Gamma_{15}}{2} & \frac{\Gamma_{18}}{2} & \frac{\Gamma_{20}}{2} & \frac{\Gamma_{21}}{2} & \left[\Gamma_6+\frac{\lambda}{p}\overline{\Pi}_6\right]
\end{vmatrix} = 0$$

Eqn. (13)

The largest eigenvalue of the determinant in Eqn. (13) will yield the smallest buckling load p_{cr}. Denoting this eigenvalue by $\pi^2 k$,

$$\pi^2 k = \lambda/p_{cr} = \frac{\pi^4 D}{L^2}/p_{cr} \qquad \ldots\ldots\ldots\ldots (14)$$

the following formula for the critical load is obtained:

$$p_{cr} = k \frac{\pi^2 D}{L^2} \qquad \ldots\ldots\ldots\ldots (15)$$

Formula (15) has the same form as the familiar formula for the critical load of a plate uniformly loaded on the top and the bottom edges (see Ref. (1), page 329, Eqn. 213). The constant k in Eqn. (15), is, of course, different from the equivalent constant in that relatively elementary case and depends both on the dimensions of the plate (h/L) and the ratio of the width 2B of the strip loading to L (but not on the thickness of the plate).

II. Numerical Evaluation and Results.

As is seen from Eqn. (15), in order to obtain the critical load for a plate as shown in Fig. 1, the value of the constant k corresponding to the dimensions of the plate and the width of the strip loading must be known. The work connected with the evaluation of this constant in each case by conventional means is prohibitive. However, it would be possible to carry out appropriate computations on electronic computers and subsequently to plot the computed values of k in the form of graphs which may be readily useable for design purposes.

Only nine values of k for different combinations of β and 2B, have been computed on ordinary desk computers. Before presenting the results, however, a brief discussion on the convergence of the series in Eqn. (12e) as well as on the method of computing the largest eigenvalue of the matrix in Eqn. (13), will be made.

a) Convergence of the Series.

The elements of the matrix in Eqn. (13) are each given by an infinite series similar to that in Eqn. (12e). The series for each of the 21 elements of the matrix are different in form, but the summation in all of them is carried on n, as in Eqn. (12e). The series and their convergence are more fully discussed in footnote 1. The following are the results of that discussion:

1) All 21 expressions for Γ are alternating infinite series.
2) Convergence is faster for larger values of both β and 2B, the influence of β on the convergence being more pronounced than that of 2B.
3) The convergence for numerical evaluation is generally fair. For example, for the cases computed in this paper, the number of terms necessary to obtain an accuracy of 0.1% in the summation of the series were as follows:
   a) $\beta = 2$, one to four terms,
   b) $\beta = 1$, one to six terms,
   c) $\beta = 1/4$, two to eight terms.
   Variation in the number of terms corresponding to each value of β as given above, depended on the value of 2B and on the type of the series, i.e. on the subscript of Γ.

b) Evaluation of the Eigenvalues.

Numerical values of the largest eigenvalue of such matrices can be computed with relative ease by the iteration method.[6] For the cases computed in this paper, four to six iterations were necessary to achieve an accuracy of 1% in the eigenvalues.

c) Results of Numerical Computations.

The nine cases for which k has been computed, are shown in Table I:

Table I

Case No.		2B/L	Computed value of k
1	2	1/65	378.00
2	2	1/20	116.30
3	2	1	10.67
4	1	1/65	216.00
5	1	1/20	67.30
6	1	1	6.20
7	1/4	1/65	559.00
8	1/4	1/20	169.20
9	1/4	1	26.60*

As was already mentioned, in order to obtain one value of k it is required to compute 21 infinite series—one for each element of the symmetric matrix—and then to evaluate the largest eigenvalue of the resulting numerical matrix. The summation of the infinite series for each element of the matrices for the nine cases shown in Table I was carried out until the remainder of the series in each case was less than 0.1% of the sum of the computed first terms. If a numerical error had occurred in the summation for any one of the 21 elements in each matrix, it would have definitely impaired the convergence in the iteration procedure. In the first eight cases of Table I, the iteration converged to within 1 % of the final value very rapidly. In the ninth case (marked with an asterisk in Table I), however, the iterated eigenvalue oscillated within $\pm$ 8% with no indication of improvements; the reason for this may have been some undetected numerical error which had occurred in the summation of the series in one or more elements of the corresponding matrix. Hence it may be concluded that the values of k in Table I for cases 1 to 8 are accurate within 1% while for case 9, only within about 10%.

d) Graphs for Computation of Buckling Loads.

The computed values of k in Table I are plotted versus β in Fig. 2 and versus 2B/L in Fig. 3; the latter graph is plotted on a semi-logarithmic scale. Smooth curves have been drawn through the three available points for each curve. It can be demonstrated [1] that between the three plotted points, the curves have to be continuous and must possess continuous derivatives; hence, the general shape of the curves must be that drawn in Figs. 2 and 3.

A comparison of the curves in Fig. 2 with those applicable to uniformly loaded plates (Ref. (2), page 330 Fig. 172) will reveal the similarity in the curves for the two cases.

One additional curve, based on the computed values of k, is drawn in Fig. 4. It shows the variation in strength (p_{cr}) of a plate of constant depth (h_1) and with constant width ($2B_1$) of the strip loading, with the variation in the length (L). For the case shown in Fig. 4, the width ($2B_1$) was arbitrarily so chosen that for a square plate (e.e., $\beta = h_1/L_1 = 1$), $2B_1/L_1 = 1/15$. It is apparent that as the length (L) of the plate is varied, the ratio $2B_1/L$ varies accordingly. Most of the points on the curve have been interpolated from the curves in Figs. 2 and 3.

The curve in Fig. 4 has been drawn for the instructive observation that the buckling strength of plates of various lengths loaded and supported as in Fig. 1, vary very little when they are sufficiently long, say if $\beta < 1/3$.

e) Application to Plates With Supports Different From Figure 1.

A common practical case is shown in Fig. 5, where the plate is supported at the bottom corners rather than by shearing stresses along its vertical edges (Fig. 1). The curves of Figs. 2 and 3 could be applied to a plate so supported provided the plate is long enough, say $\beta < 1/3$ (and obviously if buckling at the supports is prevented). This can be explained, on the one hand, by St. Venant's principle, and on the other, by tests which will be discussed in the next section.

According to St. Venant's principle, the manner of application of the reactions at the extreme vertical edges of the plate will not materially affect the stress distribution in the region of the plate sufficiently far removed from these edges; for practical purposes, this region can be considered to lie within the middle portion of the plate at a distance h (depth of the plate) from each vertical edge. The buckling load, of course, depends on the magnitude and the distribution of the stresses in the plate.

In tests, failure of the plates was characterized by deformations out of the plane of the plates in the region directly underneath the external load. This is shown in Fig. 6. These deformations, in all tests, occurred in a region which was in the central portion of the plate; this region had a width approximately equal to the depth of the plate, as shown in Fig. 6.

For the above two reasons it seems justified to apply the derived curves to long plates supported in any manner at their vertical edges. Furthermore, it seems reasonable to expect that these curves would also apply to long plates fixed, or elastically restrained, at their vertical edges, and not necessarily hinged as was assumed in Fig. 1.

The above conclusions would not hold for short plates when $\beta > 1/3$. For such plates, the manner in which the reactions are applied and the elastic conditions at the edges, are of paramount importance. No general solution for stress distribution in plates supported as in Fig. 6 has yet been derived. Numerical results for specific cases are available, obtained by finite differences or similar methods.[7] For these cases, however, the buckling loads also would have to be determined by some numerical method, for each individual case. This was the reason for choosing a plate supported as in Fig. 1 for which there is a known stress function (Eqn. (2)), since a general solution of the buckling load in terms of the plate and load parameters was desired.

Finally it may be mentioned that the work of footnote 1, as indicated in this paper, can be extended to the buckling load determination of plate girder webs. Although some modifications in the evaluated matrices would be needed, the work already performed constitutes the bulk of the mathematical development that is required for the determination of the buckling loads for the usual cases of stiffened and unstiffened webs of plate girders. The theoretical procedure for plate girders is outlined in footnote 1.

III. Tests

a) Description of the Tests

Tests, referred to previously in the paper, have been carried out by the author at Cornell University as a part of an extensive research project on Web Crippling of Light Gage Steel Beams for the American Iron and Steel Institute. A complete description of these tests has been given in reference [8].

A sketch of a typical test specimen and its loading is shown in Figs. 7a and 7b. As may be seen, every test specimen has two vertical webs. If each of these webs is looked upon as a vertical plate, they are then in many respects similar to the case considered in this paper. The main differences between the tested plate and the theoretically treated plate are: a) in end reactions, and b) in shear stresses along the top and bottom edges. In the tested plate, due to the presence of flanges, there are horizontal shearing stresses transmitted by the flanges to the top and bottom edges which do not exist in the theoretically treated plate. Otherwise, the correspondence in the boundary conditions and in other features is very close between the two cases. This correspondence is discussed more fully in footnote 1.

The test specimens were of 16 gage sheet (0.060 in. thick), 3 to 12 inches deep and all of constant ratio of depth to length namely, $\beta = 1/4$. The width (2B) of the central bearing plate through which the external load was applied (Fig. 7a) varied within the range from 2B/L = 1/65 to 1/4.8. The steel in one half the number of the test specimens had a yield stress of about 33000 psi and in the other half of about 54000 psi.

An unavoidable phenomenon in the tests was the bending of the webs out of the vertical plane. This was caused by slight eccentricity of the external load with respect to the plane of the web due to the fact that the load was applied through the flanges of the specimens (Fig. 7a) which in turn had rounded corners at junction with the web. Radius (r) of corner bents was, r = t.

During the progress of a test at moderately high loads, but still before failure, the webs bent inwards (Fig. 7c) and deflected out of their plane. These deflections were of relatively small magnitude and extended throughout the depth of a web in the vicinity of the external load (i.e. central bearing plate in Fig. 7a). This was due, undoubtedly, to bending caused by the eccentric loading.

At failure, there was a sudden bulging of the web with large deflections under, and in the immediate vicinity of, the central bearing plate, as shown in Fig. 6.

It will be realized from the above that although the webs were subjected to bending, buckling was the governing factor in failure. Nevertheless, the presence of bending is bound to have its effect and should be borne in mind in comparing test failure loads with the theoretical buckling loads. Because of the effect of bending, one would expect higher failure loads for the higher strength steel than for the lower strength steel. Due to bending, the absolute depth (h) of the web would also have an additional effect on the failure load. Finally, the membrane action of the web (post buckling strength) should not be neglected in comparing failure loads with the theoretical buckling loads.

b) Test Results; Comparison With Theoretical Buckling Loads.

The failure loads obtained in the tests are plotted in Fig. 8 to the same scale as the theoretical curve for buckling loads. The latter is shown by a solid line and was obtained from Fig. 3. The broken lines join tested points of identical test specimens but of varying 2B/L.

Inspection of Fig. 8 will reveal the following:

1) The trend of the test failure loads is the same as that of the theoretical curve.
2) Agreement between the tests and the theoretical loads is closer for the specimen of the lower yield steel than for the higher yield steel. The agreement is closest for the 6" and the 9" deep specimens (h/t of 90 and 150, respectively) of the lower yield group specimens.

3) The theoretical curve predicts mostly buckling loads smaller than test failure loads. This is particularly true for deeper specimens of high yielding steel.

The discrepancies between the theoretical curve and the tests could be attributed to the following:

a) Difference in the experimental set-up and the theoretical case analysed.
b) Post-buckling strength.
c) Use of only six terms in Eqn. (10). Because buckling in the treated case is mostly a localised effect, greater accuracy should be expected by using more than six terms in the expansion of the expression for the buckled shape. However, addition of one or more terms to Eqn. (10) would increase considerably the mathematical work involved.

CONCLUSION

Formula for the buckling load of flat rectangular plates loaded with strip loading at one edge has been derived. This formula has been reduced to the familiar form for the buckling load of flat rectangular plates loaded uniformly along the two opposite edges; the difference between the formulae for the two cases is in the buckling coefficient k. In the formula derived in this paper, k depends on the plate dimensions and loading widths. Curves for the determination of this coefficient have been plotted and can be readily used for the design purposes.

ACKNOWLEDGMENT

The tests referred to in this note were carried out at Cornell University as part of an investigation on Web Crippling in Light Gage Steel Structural Members, under the direction of Professor George Winter. This investigation was part of a research project sponsored by the Technical Subcommittee of the Committee on Building Codes of the American Iron and Steel Institute, Milton Male, chairman, F. E. Fahy, vice-chairman, B. L. Wood, consulting engineer.

Many helpful and constructive suggestions during the preparation of this paper were made by Professors George Winter and Paul P. Bijlaard of the Structural Engineering Department at Cornell University.

REFERENCES

1. Theory of Elastic Stability, by S. Timoshenko, McGraw-Hill, 1936.
2. Karl Girkmann, Stegblechbeulung unter ortlichem Lastangriff; Akademie der Wissenschaften, Wien, Sitzungsberichte Mathematische-Naturalwissenschaften Klasse. Abteilung 2A., 1936.
3. Karl Girkmann, Stability of the Webs of Plate Girders Taking Account of Concentrated Loads; International Association for Bridge and Structural Engineering, Final Report, 1936.
4. Karl Girkmann, Stegblechbeulung, Verursacht durch ortlichen Lastangriff; Fifth International Congress for Applied Mechanics, Cambridge, Mass., 1938.

5. F. Seewald, Die Spannungen und Formanderungen von Balken mit rechteckigem Querschnitt, Abhandlungen aus dem Aerodynamischen Institut an der Tech. Hochschule Aachen, Heft 7.

6. Mathematical Methods in Engineering, Karman and Biot, McGraw-Hill 1940, page 200.

7. Stresses in Deep Beams, by L. Chow, H. D. Conway, and G. Winter, ASCE Trans. 1953, Vol. 118, page 686.

8. L. Zetlin and G. Winter: 65th and 66th Progress Reports to the American Iron and Steel Institute on Tests on Light Gage Steel Beams of Cold Formed Steel, Cornell Univ., Sept. 1952 and Jan. 1953.

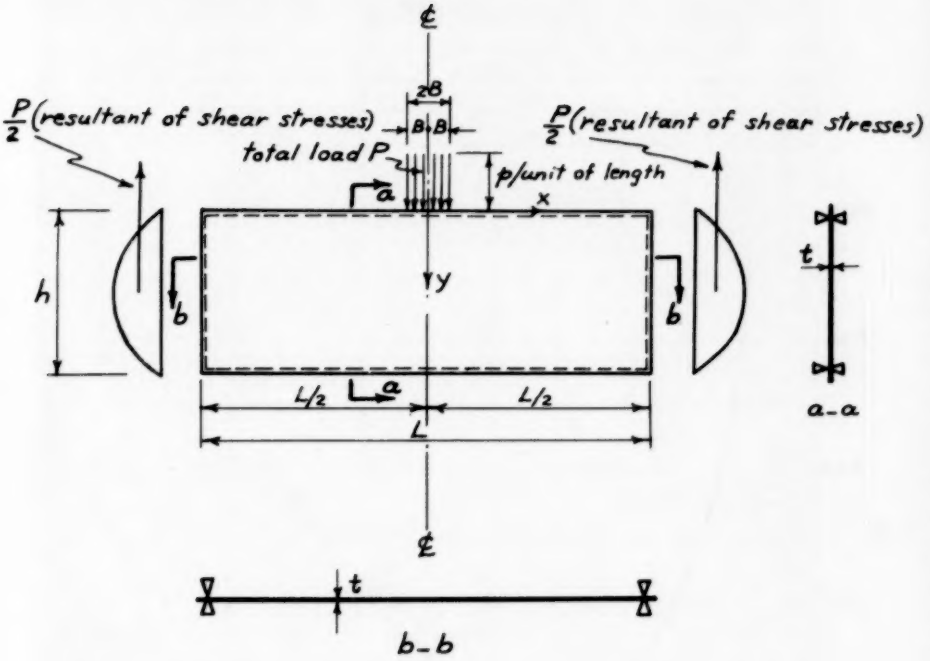
℄
2B
B B
P/2 (resultant of shear stresses)
P/2 (resultant of shear stresses)
total load P
p/unit of length
a
x
y
h
b
b
t
a-a
L/2
a
L/2
L
℄
t
b-b

FIGURE 1

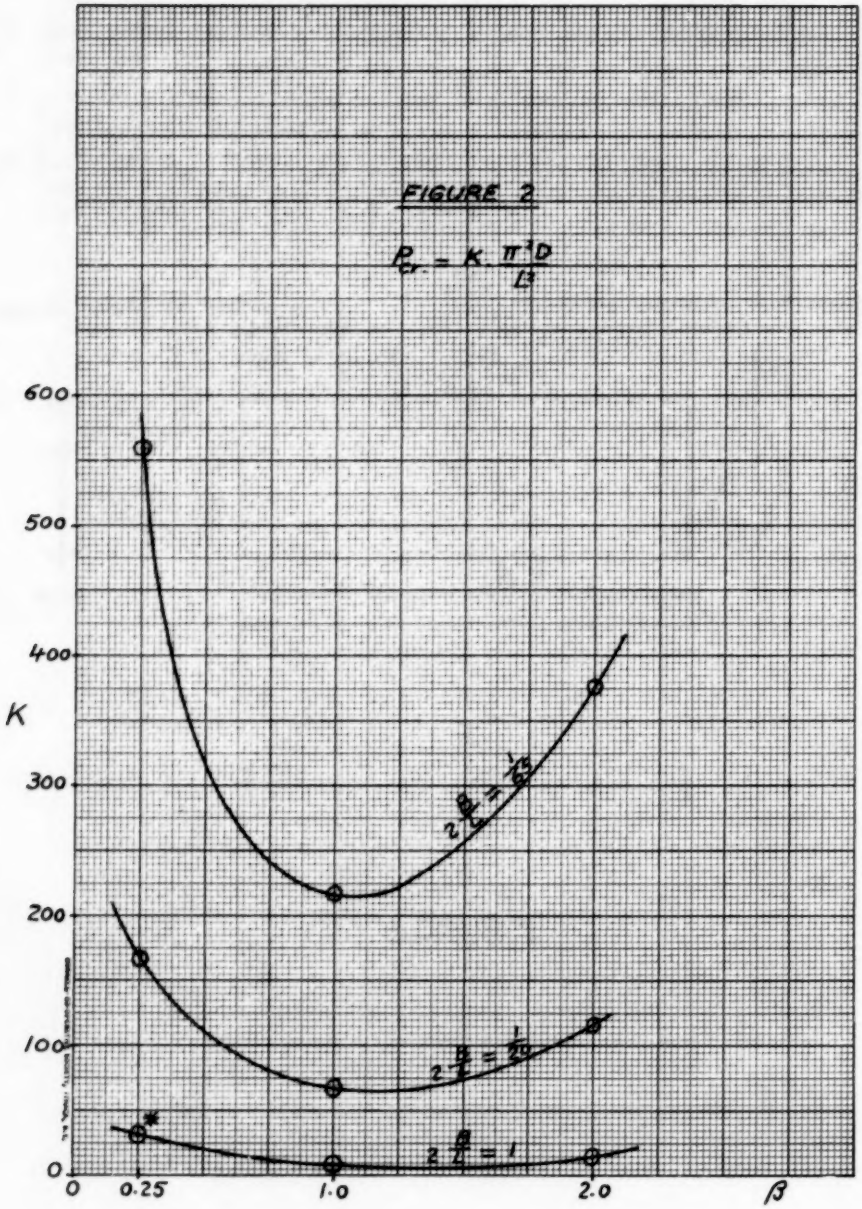
FIGURE 2
$P_{cr.} = K \frac{\pi^2 D}{L^2}$
600
500
400
K
300
200
100
0
0.25
1.0
2.0
β
$2\frac{a}{L} = \frac{1}{\sqrt{2}}$
$2\frac{a}{L} = 1$

FIGURE 3

$$P_{cr} = K \cdot \frac{\pi^2 D}{L^2}$$

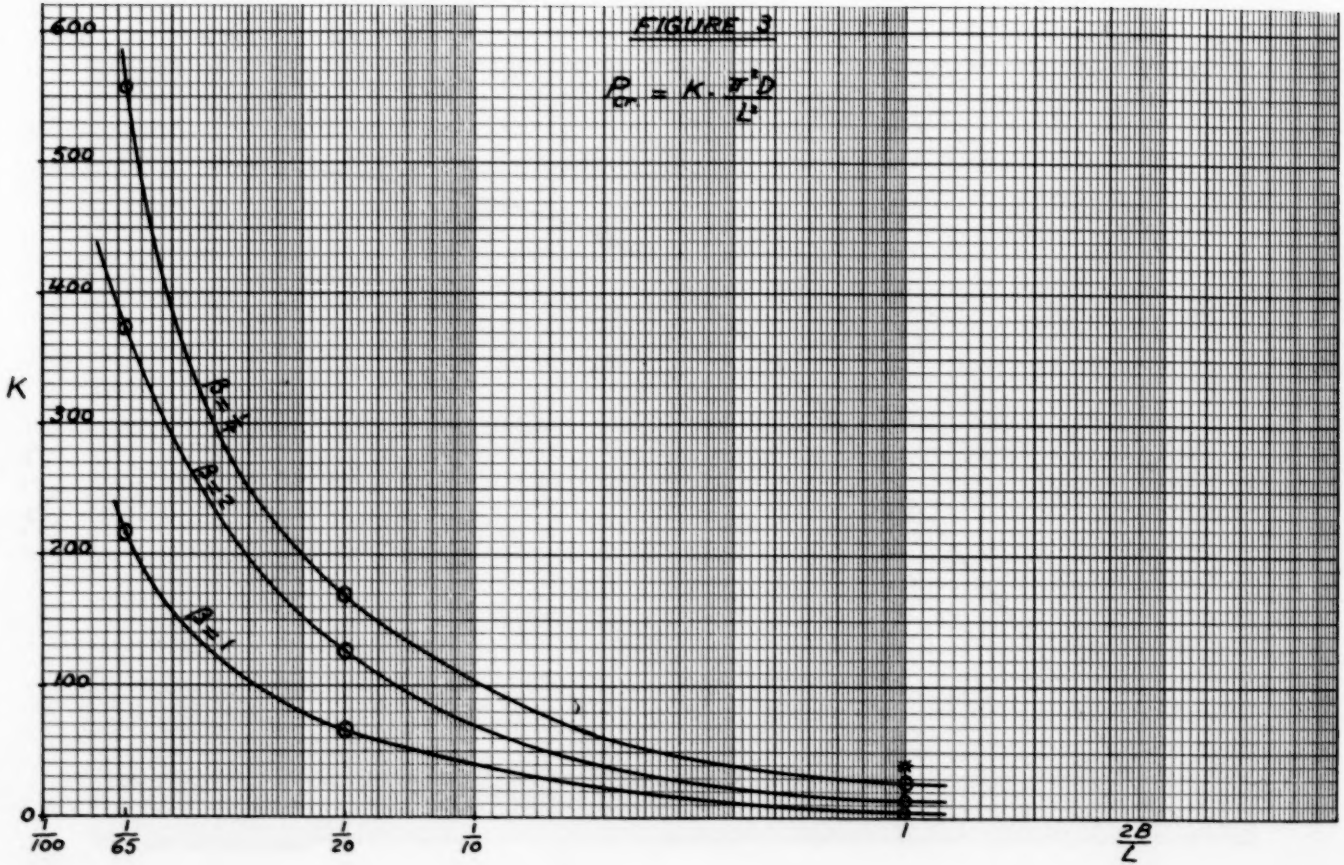

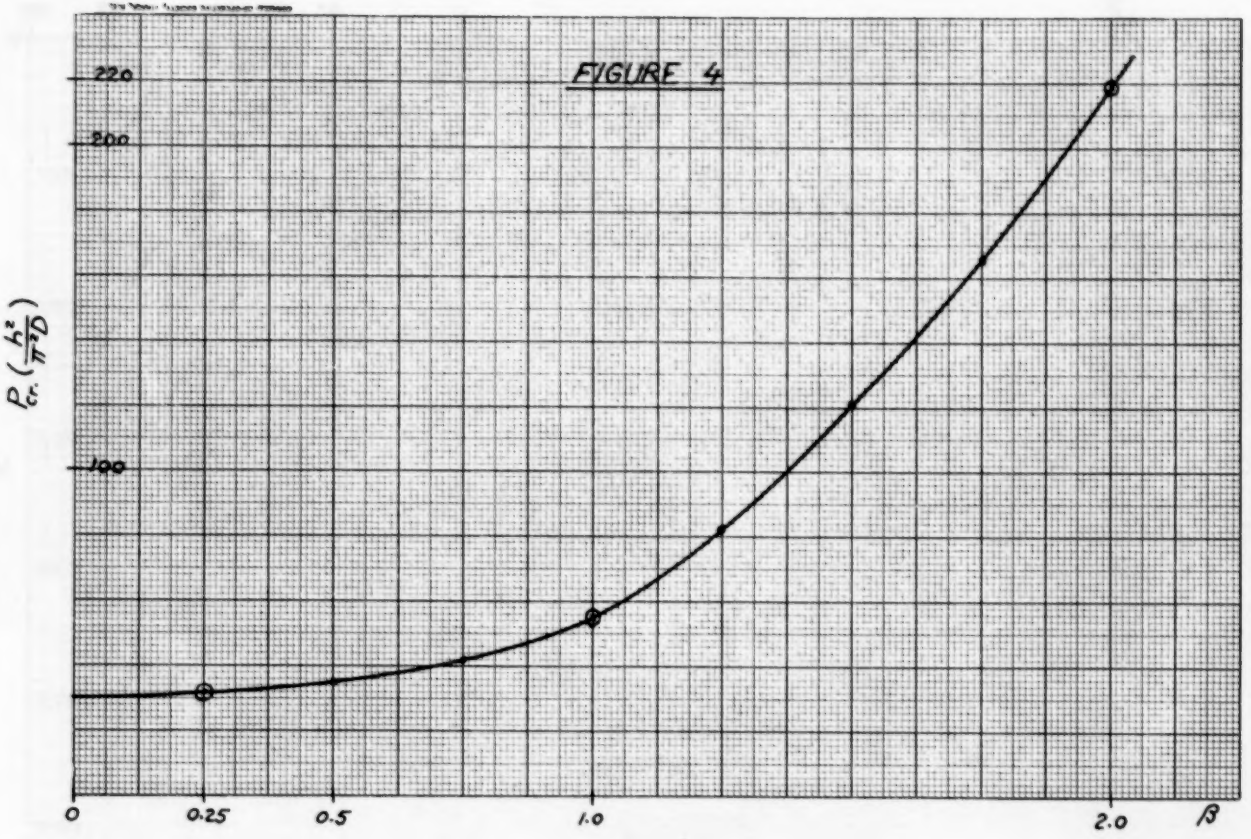
FIGURE 4
$P_{cr.}\left(\frac{h^2}{\pi^2 D}\right)$
220
200
100
0
0.25
0.5
1.0
2.0
β

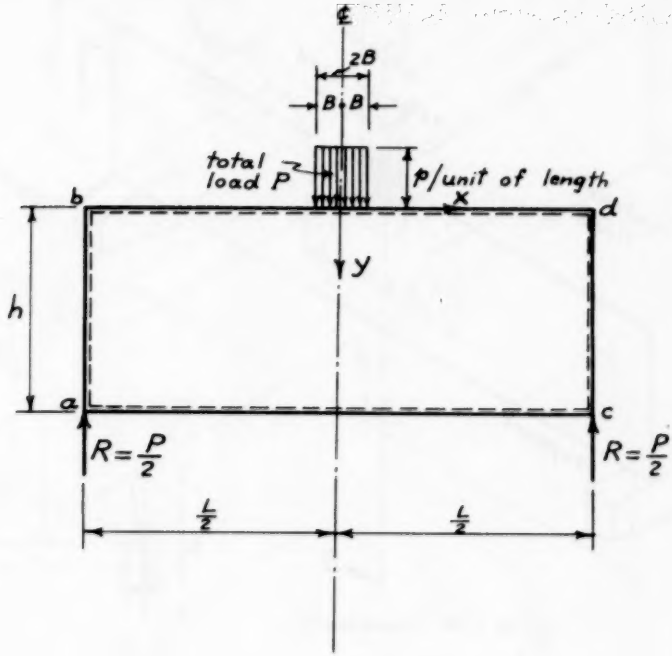

FIGURE 5

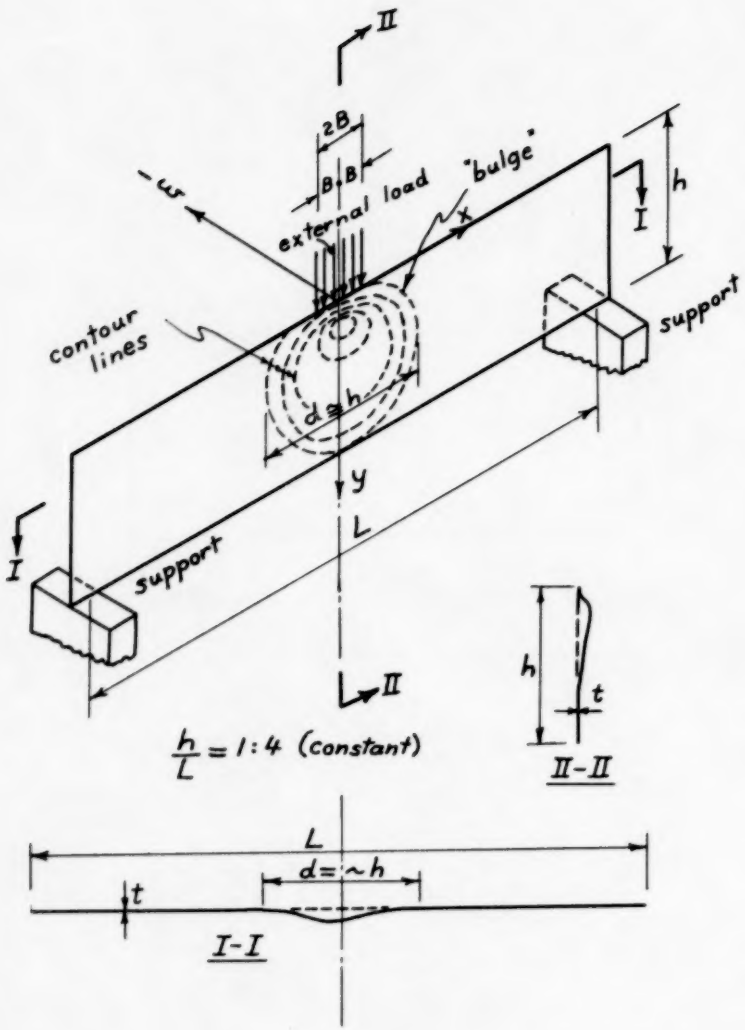
II
2B
B B
-w
external load
"bulge"
x
I
h
contour lines
support
d ≈ h
y
L
I
support
II
h
t
II-II
h/L = 1:4 (constant)
L
d ≈ h
t
I-I

FIGURE 6

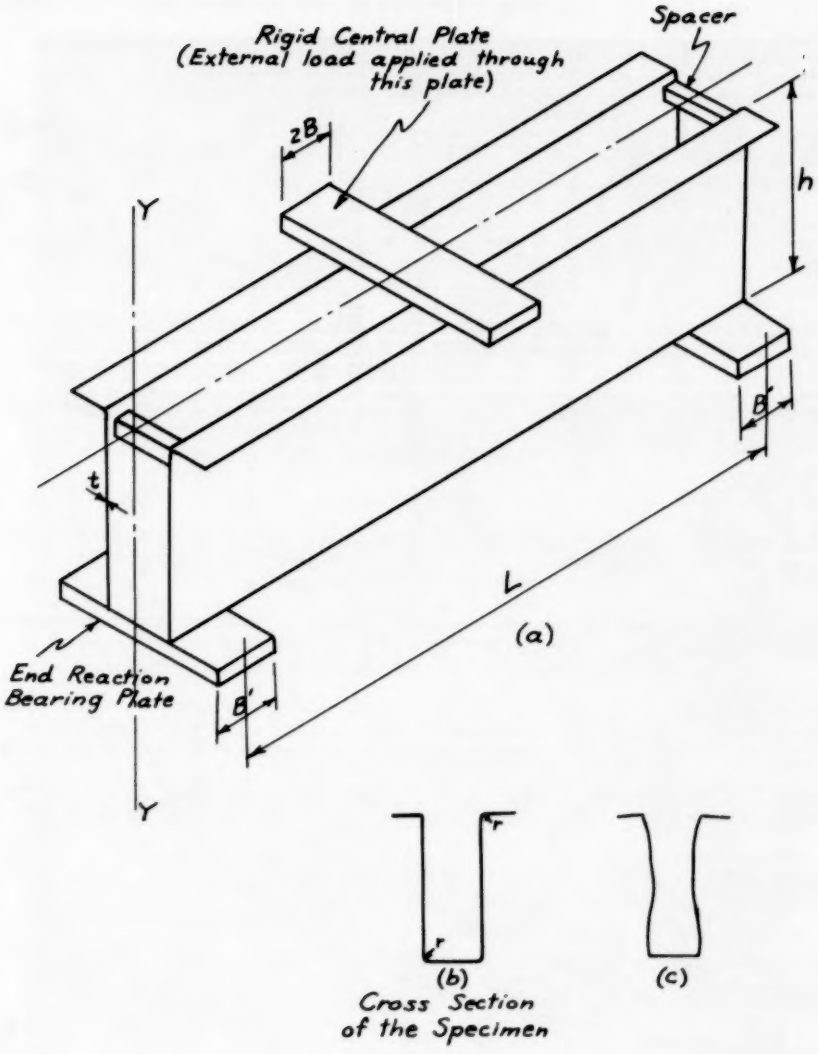
Rigid Central Plate
(External load applied through this plate)
Spacer
2B
h
Y
B'
t
L
(a)
End Reaction Bearing Plate
B'
Y
r
r
(b)
(c)
Cross Section of the Specimen

FIGURE 7

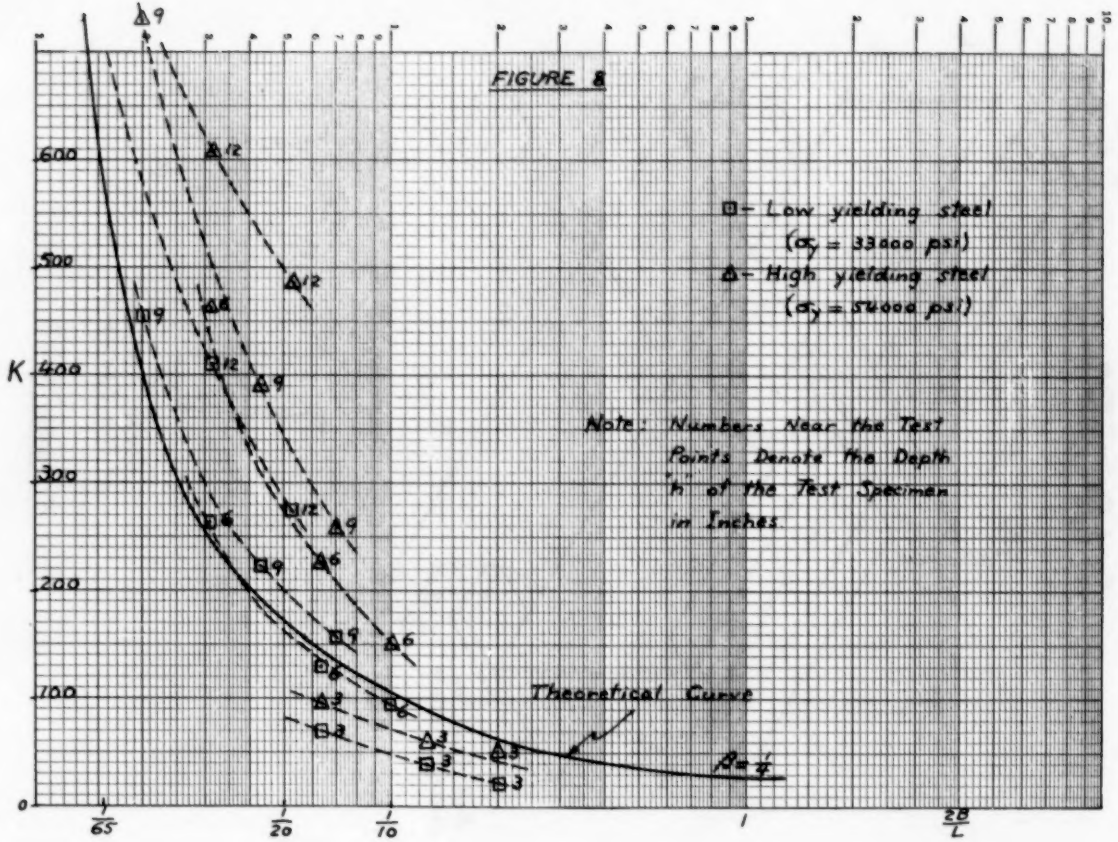
FIGURE 8
□= Low yielding steel
(σ_y = 33000 psi)
Δ= High yielding steel
(σ_y = 51000 psi)
Note: Numbers Near the Test Points Denote the Depth "h" of the Test Specimen in Inches
Theoretical Curve
β=1
K
600
500
400
300
200
100
0
1/65
1/20
1/10
1
28/L

The technical papers published in the past year are presented below. Technical-division sponsorship is indicated by an abbreviation at the end of each Paper Number, the symbols referring to: Air Transport (AT), City Planning (CP), Construction (CO), Engineering Mechanics (EM), Highway (HW), Hydraulics (HY), Irrigation and Drainage (IR), Power (PO), Sanitary Engineering (SA), Soil Mechanics and Foundations (SM), Structural (ST), Surveying and Mapping (SU), and Waterways (WW) divisions. For titles and order coupons, refer to the appropriate issue of "Civil Engineering" or write for a cumulative price list.

VOLUME 80 (1954)

SEPTEMBER: 484(ST), 485(ST), 486(ST), 487(CP)[c], 488(ST)[c], 489(HY), 490(HY), 491(HY)[c], 492(SA), 493(SA), 494(SA), 495(SA), 496(SA), 497(SA), 498(SA), 499(HW), 500(HW), 501(HW)[c], 502(WW), 503(WW), 504(WW)[c], 505(CO), 506(CO)[c], 507(CP), 508(CP), 509(CP), 510(CP), 511(CP).

OCTOBER: 512(SM), 513(SM), 514(SM), 515(SM), 516(SM), 517(PO), 518(SM)[c], 519(IR), 520(IR), 521(IR), 522(IR)[c], 523(AT)[c], 524(SU), 525(SU)[c], 526(EM), 527(EM), 528(EM), 529(EM), 530(EM)[c], 531(EM), 532(EM)[c], 533(PO).

NOVEMBER: 534(HY), 535(HY), 536(HY), 537(HY), 538(HY)[c], 539(ST), 540(ST), 541(ST), 542(ST), 543(ST), 544(ST), 545(SA), 546(SA), 547(SA), 548(SM), 549(SM), 550(SM), 551(SM), 552(SA), 553(SM)[c], 554(SA), 555(SA), 556(SA), 557(SA).

DECEMBER: 558(ST), 559(ST), 560(ST), 561(ST), 562(ST), 563(ST)[c], 564(HY), 565(HY), 566(HY), 567(HY), 568(HY)[c], 569(SM), 570(SM), 571(SM), 572(SM)[c], 573(SM)[c], 574(SU), 575(SU), 576(SU), 577(SU), 578(HY), 579(ST), 580(SU), 581(SU), 582(Index).

VOLUME 81 (1955)

JANUARY: 583(ST), 584(ST), 585(ST), 586(ST), 587(ST), 588(ST), 589(ST)[c], 590(SA), 591(SA), 592(SA), 593(SA), 594(SA), 595(SA)[c], 596(HW), 597(HW), 598(HW)[c], 599(CP), 600(CP), 601(CP), 602(CP), 603(CP), 604(EM), 605(EM), 606(EM)[c], 607(EM).

FEBRUARY: 608(WW), 609(WW), 610(WW), 611(WW), 612(WW), 613(WW), 614(WW), 615(WW), 616(WW), 617(IR), 618(IR), 619(IR), 620(IR), 621(IR)[c], 622(IR), 623(IR), 624(HY)[c], 625(HY), 626(HY), 627(HY), 628(HY), 629(HY), 630(HY), 631(HY), 632(CO), 633(CO).

MARCH: 634(PO), 635(PO), 636(PO), 637(PO), 638(PO), 639(PO), 640(PO), 641(PO)[c], 642(SA), 643(SA), 644(SA), 645(SA), 646(SA), 647(SA)[c], 648(ST), 649(ST), 650(ST), 651(ST), 652(ST), 653(ST), 654(ST)[c], 655(SA), 656(SM)[c], 657(SM)[c], 658(SM)[c].

APRIL: 659(ST), 660(ST), 661(ST)[c], 662(ST), 663(ST), 664(ST)[c], 665(HY)[c], 666(HY), 667(HY), 668(HY), 669(HY), 670(EM), 671(EM), 672(EM), 673(EM), 674(EM), 675(EM), 676(EM), 677(EM), 678(HY).

MAY: 679(ST), 680(ST), 681(ST), 682(ST)[c], 683(ST), 684(ST), 685(SA), 686(SA), 687(SA), 688(SA), 689(SA)[c], 690(EM), 691(EM), 692(EM), 693(EM), 694(EM), 695(EM), 696(PO), 697(PO), 698(SA), 699(PO)[c], 700(PO), 701(ST)[c].

JUNE: 702(HW), 703(HW), 704(HW)[c], 705(IR), 706(IR), 707(IR), 708(IR), 709(HY)[c], 710(CP), 711(CP), 712(CP), 713(CP)[c], 714(HY), 715(HY), 716(HY), 717(HY), 718(SM)[c], 719(HY)[c], 720(AT), 721(AT), 722(SU), 723(WW), 724(WW), 725(WW), 726(WW)[c], 727(WW), 728(IR), 729(IR), 730(SU)[c], 731(SU).

JULY: 732(ST), 733(3T), 734(ST), 735(ST), 736(ST), 737(PO), 738(PO), 739(PO), 740(PO), 741(PO), 742(PO), 743(HY), 744(HY), 745(HY), 746(HY), 747(HY), 748(HY)[c], 749(SA), 750(SA), 751(SA), 752(SA)[c], 753(SM), 754(SM), 755(SM), 756(SM), 757(SM), 758(CO)[c], 759(SM)[c], 760(WW)[c].

AUGUST: 761(BD), 762(ST), 763(ST), 764(ST), 765(ST)[c], 766(CP), 767(CP), 768(CP), 769(CP), 770(CP), 771(EM), 772(EM), 773(SA), 774(EM), 775(EM), 776(EM)[c], 777(AT), 778(AT), 779(SA), 780(SA), 781(SA), 782(SA)[c], 783(HW), 784(HW), 785(CP), 786(ST).

SEPTEMBER: 787(PO), 788(IR), 789(HY), 790(HY), 791(HY), 792(HY), 793(HY), 794(HY)[c], 795(EM), 796(EM), 797(EM), 798(EM), 799(EM)[c], 800(WW), 801(WW), 802(WW), 803(WW), 804(WW), 805(WW), 806(HY), 807(PO)[c], 808(IR)[c].

c. Discussion of several papers, grouped by Divisions.

AMERICAN SOCIETY OF CIVIL ENGINEERS

OFFICERS FOR 1955

PRESIDENT

WILLIAM ROY GLIDDEN

VICE-PRESIDENTS

Term expires October, 1955:
ENOCH R. NEEDLES
MASON G. LOCKWOOD

Term expires October, 1956:
FRANK L. WEAVER
LOUIS R. HOWSON

DIRECTORS

Term expires October, 1955:
CHARLES B. MOLINEAUX
MERCEL J. SHELTON
A. A. K. BOOTH
CARL G. PAULSEN
LLOYD D. KNAPP
GLENN W. HOLCOMB
FRANCIS M. DAWSON

Term expires October, 1956:
WILLIAM S. LaLONDE, JR.
OLIVER W. HARTWELL
THOMAS C. SHEDD
SAMUEL B. MORRIS
ERNEST W. CARLTON
RAYMOND F. DAWSON

Term expires October, 1957:
JEWELL M. GARRELTS
FREDERICK H. PAULSON
GEORGE S. RICHARDSON
DON M. CORBETT
GRAHAM P. WILLOUGHBY
LAWRENCE A. ELSENER

PAST-PRESIDENTS

Members of the Board

WALTER L. HUBER
DANIEL V. TERRELL

EXECUTIVE SECRETARY
WILLIAM H. WISELY

TREASURER
CHARLES E. TROUT

ASSISTANT SECRETARY
E. L. CHANDLER

ASSISTANT TREASURER
CARLTON S. PROCTOR

PROCEEDINGS OF THE SOCIETY

HAROLD T. LARSEN
Manager of Technical Publications

DEFOREST A. MATTESON, JR.
Editor of Technical Publications

PAUL A. PARISI
Assoc. Editor of Technical Publications

COMMITTEE ON PUBLICATIONS

SAMUEL B. MORRIS, *Chairman*

JEWELL M. GARRELTS, *Vice-Chairman*

GLENN W. HOLCOMB
OLIVER W. HARTWELL
ERNEST W. CARLTON
DON M. CORBETT